Getting the Lines Crossed—How a Three-Phase Series Fault Caused a Sequence of Relay Operations

Marcel Taberer, Ryan McDaniel, and Jon Larson
Schweitzer Engineering Laboratories, Inc.

Presented at the
59th Annual Minnesota Power Systems Conference
Saint Paul, Minnesota
November 7–9, 2023

Previously presented at the
76th Annual Georgia Tech Protective Relaying Conference, May 2023

Originally presented at the
76th Annual Conference for Protective Relay Engineers, March 2023

Getting the Lines Crossed—How a Three-Phase Series Fault Caused a Sequence of Relay Operations

Marcel Taberer, Ryan McDaniel, and Jon Larson, *Schweitzer Engineering Laboratories, Inc.*

***Abstract*—During a planned outage, a utility replaced the line entrance conductors on a 120 kV breaker. During the installation, operating personnel inadvertently crossed all three phases on the incoming side of the breaker. Unaware of the cross-connection, the operating personnel closed the breaker to return the equipment back to service. This resulted in an unusual fault, cross-connecting all three phases between two sources. As a result of this unintentional man-made fault, line protection and transformer differential relays operated unexpectedly.**

The cross-connection occurred at a breaker location, and an adjacent line relay, which was part of a directional comparison blocking (DCB) scheme, operated. A nearby transformer differential relay protecting a 15 MVA delta-wye transformer also operated, although this fault was not in its zone of protection.

In this paper, we discuss why the transmission line distance relays operated for this unique fault by analyzing the event reports from the relays involved and discuss how advancements in distance element polarization help maintain security for this fault. We also analyze the transformer relay operation and provide solutions for transformer differential security for this fault.

I. Introduction

On one eventful day, two utilities had a planned outage on a shared 120 kV line so that entrance conductors could be replaced on one of the breakers at the substation. A one-line diagram of the system is shown in Fig. 1. Line 1 is a short line with line current differential (87L) deployed as primary protection on Relays 3 and 4 and phase and ground distance protection configured as a backup. Relays 1 and 2 on Line 2 are configured with phase and ground distance protection using a directional comparison blocking (DCB) scheme as the primary protection. There is a substation with a 15 MVA delta-wye transformer supplying radial feeders located in between the two lines. The phase differential (87R) with second-harmonic restraint is configured on Relay 5 to protect the transformer.

During the outage, operating personnel inadvertently swapped all three phases across Breaker A on Line 1, as shown in Fig. 1. When Breaker A closed, an unusual fault occurred, cross-connecting all three phases between Source 1 and Source 2. The 87L protection on Line 1 issued a trip and opened Breakers A and B.

Relay 1 and Relay 2 were deployed using a DCB scheme. Relay 1 initially saw the series fault in the reverse direction, while Relay 2 saw the series fault in the forward direction. Line 2 momentarily remained energized because Relay 1 initially sent a blocking signal to Relay 2. That was short-lived, and after 2 cycles, Relay 1 stopped sending a blocking signal to Relay 2. Upon loss of the block signal from Relay 1, Relay 2 was allowed to operate the Zone 2 phase distance (Z2) element, which opened Breaker D, resulting in an outage on Line 2.

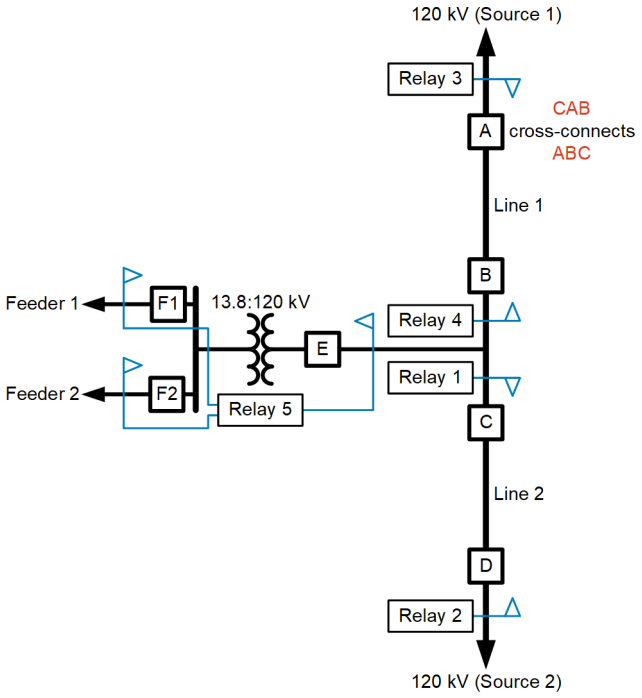

Fig. 1. One-Line Diagram of the System

In addition to the line protection operations, Relay 5, which is a transformer differential relay, operated for this series fault, due to significant inrush current, and opened Breaker E.

Each utility asked some fundamental questions when diving into the nuts and bolts of this man-made fault:

- Why did Relay 1 stop sending a block signal to Relay 2 on Line 2, allowing Z2 on Relay 2 to trip Breaker D?
- Why was there inrush current captured on Relay 5 for this series fault? Why did Relay 5 not restrain the 87R element and prevent a trip during this inrush current?

In this paper, we discuss concepts relating to cross-connecting three phases between two sources. We discuss transmission line directional element and distance element behavior during this unique fault type using theory and field data. We show how advancements in methods of polarization help maintain a blocking signal for relays using a DCB scheme on remote lines for out-of-section three-phase cross-connect faults. We then show the field event for the transformer and discuss the reason for inrush current captured by Relay 5. We explain why the transformer differential relay operated in the presence of inrush current and show how advancements in

transformer differential relaying increase security in challenging transformer inrush cases.

II. Three-Phase Cross-Connect Fault Discussion

Reference [1] details a two-phase cross-connect fault, which is an unbalanced series fault in which positive- and negative-sequence networks are present. A three-phase cross-connection presents a balanced series fault. As such, the only concern is the positive-sequence network shown in Fig. 2. In this example, the right source represents ABC phasing and the positive-sequence voltage (VR1) is shown as 1∠0. There are two possible ways to create a three-phase cross-connect to an ABC source: BCA or CAB. In this example, we chose CAB and made the positive-sequence voltage on the left source (VS1) equal to Phase C (1∠120). In this section, all units of measurement are in per unit (pu).

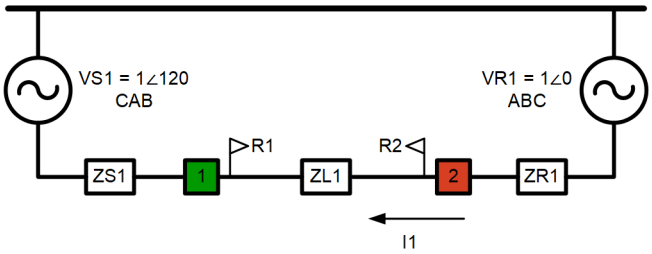

Fig. 2. Positive-Sequence Network for an Example Three-Phase Cross-Connect Fault

Initially, Breaker 1 is open and Relays R1 and R2, which are connected to line potential transformers (PTs), measure a pre-fault positive-sequence voltage equal to 1∠0. This voltage is referred to as $V1_{MEM}$ in subsequent figures and equations.

When Breaker 1 closes, a series fault develops in which the positive-sequence current seen by R2 (I1R2) is defined in (1). The positive-sequence current seen at R1 (I1R1) is the negation of the current at R2 due to CT polarity, as shown in (2). We note that the numerator of (1) evaluates to √3∠–30 for the system shown in Fig. 2.

$$I1R2 = \frac{VR1 - VS1}{ZS1 + ZL1 + ZR1} \tag{1}$$

$$I1R1 = -I1R2 \tag{2}$$

The voltages developed at R1 and R2 can be defined in (3) and (4), respectively.

$$V1R1 = \left(\frac{ZS1 + (ZL1 + ZR1) \bullet 1\angle 120}{ZS1 + ZL1 + ZR1} \right) \tag{3}$$

$$V1R2 = \left(\frac{ZS1 + ZL1 + ZR1 \bullet 1\angle 120}{ZS1 + ZL1 + ZR1} \right) \tag{4}$$

To visualize the phasor relationship that we expected for our example cross-connect fault, we solved (1) through (4) with ZS1 = ZR1 = ZL1 = 1∠90. We use this example system throughout the paper to illustrate the concepts of this fault type.

The results for (1) through (4) are plotted in Fig. 3 with R1 phasors on the left and R2 phasors on the right. The magnitudes of (1) through (4) are all 1/√3.

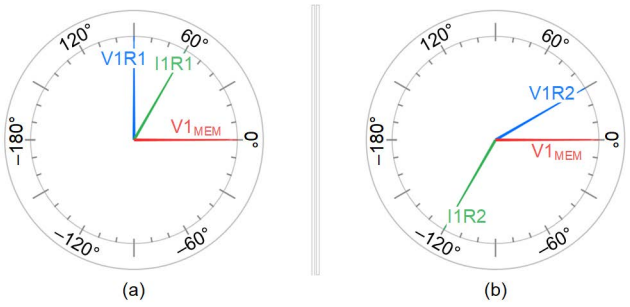

Fig. 3. R1 (a) and R2 (b) Phasors for the Example Three-Phase Cross-Connect Fault

Based on this discussion and the angular relationships shown in Fig. 3, we can make the following observations:

- The positive-sequence current (I1R2) lags the positive-sequence pre-fault memory voltage ($V1_{MEM}$) by 120 degrees at Relay R2, rather than the expected 90 degrees for this inductive system. This is because the driving voltage from (1) lags $V1_{MEM}$ by 30 degrees. At R1, the positive-sequence current (I1R1) leads $V1_{MEM}$ by 60 degrees.
- The fault voltage at Relay 2 (V1R2) shifts +30 degrees from $V1_{MEM}$. The fault voltage at Relay 1 (V1R1) shows an even greater shift of +90 degrees. Since R1 is closer to the 1∠120 source voltage than R2, there will be a larger phase angle shift at R1.

A. Positive-Sequence Polarizing Voltage

Distance and directional elements typically use $V1_{MEM}$ for polarization to maintain security and dependability for close-in three-phase faults [2]. Other benefits to using $V1_{MEM}$, such as adaptability to load, increased fault resistance coverage, and single-pole-open security, are described in [2].

Fig. 3 and subsequent figures in this section show the $V1_{MEM}$ phasor at fault initiation when $V1_{MEM}$ is equal to the pre-fault value of V1 ($V1_{PRE}$). However, as we explain later, it is not wise for $V1_{MEM}$ to equal $V1_{PRE}$ indefinitely. Therefore, over time, $V1_{MEM}$ moves closer to the fault value of V1. One method of accomplishing this type of $V1_{MEM}$ response is to use an infinite input response filter, as defined in [3]. The general formula for this implementation is shown in (5).

$$V1_{MEM} = \frac{1}{n} \bullet V1_{Current} - \frac{n-1}{n} \bullet V1_{MEM\,\frac{1}{2}\text{ cycle old}} \tag{5}$$

From this, it is clear that $V1_{MEM}$ is made up of two weighted components: the current value of V1 ($V1_{Current}$) and the 1/2-cycle-old value of $V1_{MEM}$ (which can be referred to as the memory component of $V1_{MEM}$). For n = 1, $V1_{MEM}$ has no memory component and is equal to $V1_{Current}$. In this case, $V1_{MEM}$ is only equal to the pre-fault voltage just prior to the fault, not during the fault. For large values of n, $V1_{MEM}$ is almost completely a memory component. In this case, $V1_{MEM}$ is equal to $V1_{PRE}$ for a long time after a fault has occurred. Small values of n produce a short duration memory action and therefore have a short time constant. Large values of n produce a long duration memory action and therefore have a long time constant. The

relay designer needs to find a middle ground for n to balance security with dependability.

Generally, the most demanding dependability use case for $V1_{MEM}$ is a close-in reverse fault in which the reverse pilot blocking distance element must send a blocking signal continuously to a remote relay for at least the amount of time it takes the external fault to be cleared by primary relaying. Without memory, the available voltage signal to polarize the reverse distance element goes to zero and, thus, the reverse-reaching element does not assert and fails to send a block signal to the remote overreaching pilot tripping element. When this happens, a false trip in a DCB scheme occurs. In this case, n should be large enough to maintain the $V1_{MEM}$ signal long enough to maintain security of the DCB scheme.

Generally, the most demanding security consideration for $V1_{MEM}$ is an abrupt change in frequency. If $V1_{MEM}$ is heavily weighted toward the memory component (i.e., where n is large), then $V1_{MEM}$ retains the frequency information prior to the disturbance and begins to slip from the new system frequency [4]. This can cause distance elements to misoperate and can be a concern, especially near systems with little to no rotating inertia [5]. In this case, n should be small to allow $V1_{MEM}$ to closely track current system conditions.

The relays in service at the time of the three-phase cross-connect fault implement two time constants depending on the magnitude of the V1 voltage during the fault. For severe depressions in V1 voltage due to a close-in three-phase fault (i.e., less than 10 percent of the system nominal voltage), a long memory time constant (i.e., a large n) is used to maintain distance element operation when very little V1 is available. For smaller depressions in V1 voltage, a shorter time constant (i.e., a small n) is used. This implementation requires modest processing power and allows for a good balance in dependability and security for traditional faults.

In Fig. 4, we show the angle difference between $V1_{MEM}$ and $V1_{PRE}$ over a period of 300 ms for the memory voltage implementation described in [3] after an abrupt +90-degree shift in V1. In Fig. 4, we plot a short time constant curve (short TC) and a long time constant curve (long TC).

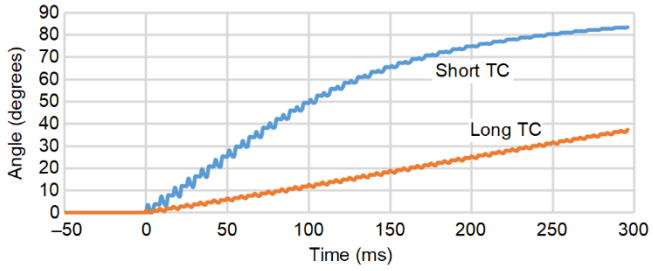

Fig. 4. Ang($V1_{MEM}$) – Ang($V1_{PRE}$) for 300 ms After a +90-Degree Phase Shift

Prior to the shift, $V1_{MEM}$ is in phase with $V1_{PRE}$. At t = 0, the $V1_{MEM}$ phase angle begins to move away from $V1_{PRE}$ and toward the new phase angle of 90 degrees. In Fig. 4, focusing on the short time constant, $V1_{MEM}$ shifts +30 degrees in about 50 ms and shifts +60 degrees in about 125 ms. At 300 ms, $V1_{MEM}$ is near the 90-degree mark, indicating that the memory component has nearly expired.

In a three-phase cross-connect fault, the V1 voltage magnitude does not depress enough to engage the long time constant memory voltage and the shorter memory time constant is engaged. Recall that in this example, the V1 voltage magnitude at each relay is at 0.57 pu ($1/\sqrt{3}$) of the nominal system voltage.

As explained later, a longer memory aids in security for a three-phase cross-connect fault as it allows directional elements and distance elements to maintain security in a DCB scheme.

B. Directional Element Evaluation

The large shift in the fault voltage phase angle can challenge directional element security when the memory component of the polarizing signal expires. To analyze this, we evaluate the torque of the directional element for this balanced series fault when memory voltage is fully engaged ($T32P_{MEM}$) (6) and when the memory component of $V1_{MEM}$ has fully expired ($T32P_{SELF}$) (7). A positive torque is a forward declaration, while a negative torque is a reverse declaration. The term $I1_{REPLICA}$ is equal to I1 • (1∠ZL1). This means that $I1_{REPLICA}$ leads I1 by 90 degrees. Equation (6) represents the directional decision that the relay initially makes for this fault, while (7) represents the directional decision that the relay makes once the memory component of $V1_{MEM}$ has expired. Throughout the remainder of the paper, the asterisk symbol (*) used in (6) and (7) is the complex conjugate operator.

$$T32P_{MEM} = RE\left[\left(I1_{REPLICA}\right)\bullet\left(V1_{MEM}\right)^*\right] \quad (6)$$

$$T32P_{SELF} = RE\left[\left(I1_{REPLICA}\right)\bullet\left(V1\right)^*\right] \quad (7)$$

If the voltage signals (i.e., $V1_{MEM}$ and V1) in (6) and (7) are more than 90 degrees from the current signal ($I1_{REPLICA}$), then the torque produced is negative and the relay declares a reverse fault. If the voltage signals in (6) and (7) are less than 90 degrees from $I1_{REPLICA}$, the torque produced is positive and the relay declares a forward fault. We create a perpendicular line (DIR) to the replica current (named $I1R1_{REPLICA}$ for Relay R1 and $I1R2_{REPLICA}$ for Relay R2 in Fig. 5) in the phasor view that indicates directionality based on the relative phase angle of the applied voltage signal.

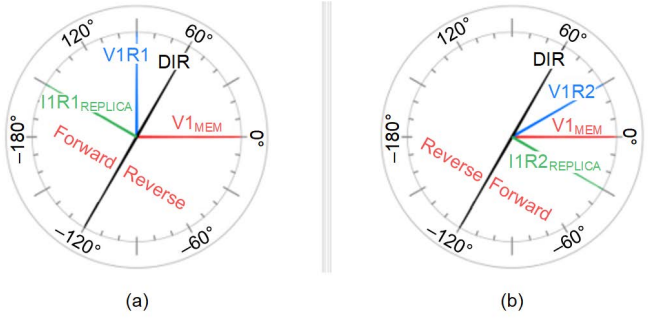

Fig. 5. Positive-Sequence Directional Element Evaluation for R1 (a) and R2 (b) During the Example Three-Phase Cross-Connect Fault

Initially, R1 declares this fault reverse since $V1_{MEM}$ is –150 degrees from $I1R1_{REPLICA}$ as (6) evaluates to a negative number. R2 initially declares this fault forward since $V1_{MEM}$ is 30 degrees from $I1R2_{REPLICA}$, and (6) evaluates to a positive number.

When the memory component of $V1_{MEM}$ expires, the directional decision at Relay R2 remains forward as V1R2 is still less than 90 degrees from $I1R2_{REPLICA}$ and (7) evaluates to a positive number. However, the directional decision at Relay R1 changes from reverse to forward as V1R1 is less than 90 degrees from $I1R1_{REPLICA}$ and (7) evaluates to a positive number. Fig. 5 shows that directionality at R1 changes when $V1_{MEM}$ moves greater than +60 degrees. It is clear from Fig. 4 that it takes about 125 ms for $V1_{MEM}$ to travel +60 degrees from its pre-fault position using a short time constant.

If there is a communications-assisted tripping scheme protecting the line, R1 and R2 are initially secure while the memory voltage is available. However, after about 125 ms, the scheme loses directional security and R1 and R2 may trip their breakers, even if the breaker that initially created the cross-connect condition is external to the line. Ideally, the memory voltage is present long enough on adjacent lines from the cross-connect closing breaker to provide security in communications-assisted schemes.

While this simple example illustrates potential security issues with communications-assisted tripping schemes, not all systems have a security concern during a cross-connect condition. For example, if the angle of V1R1 is less than 60 degrees from $V1_{MEM}$, Relay R1 declares a reverse fault regardless of whether or not memory voltage is available. In Appendix A, we offer calculations to compute the system requirements for R1 and R2 to declare a forward direction after the memory component of $V1_{MEM}$ has expired. The results are shown for R1 in (8) and R2 in (9).

$$ZR1 + ZL1 > ZS1 \tag{8}$$

$$ZS1 + ZL1 > ZR1 \tag{9}$$

These formulas show that R1 and R2 declare forward when the impedance in front of the relay is greater than the impedance behind it. This condition is true for both relays when ZL1 is large relative to ZS1 and ZR1.

If ZR1 + ZL1 = ZS1, then R1 is located at the electrical center of this simple system. Using (3), it is clear that the value of V1 seen by R1 is 0.5∠60. This is the lowest V1 magnitude on the system for this fault type and is important when considering switch-onto-fault (SOTF) settings discussed later in this paper.

C. *Distance Element Evaluation*

In the preceding section, the focus was on directionality, which helps identify the potential security issues with this three-phase series fault. However, distance elements typically operate for balanced faults on a transmission system. In this section, we extend the discussion to include positive-sequence voltage memory-polarized distance elements. The following discussion is more precise in explaining the expected relay behavior during a balanced series fault but is more complex than directional analysis.

The equation for a memory-polarized distance element, which operates only on positive-sequence quantities to detect balanced faults, is shown in (10). In practice, balanced faults are detected with traditional faulted phase loop quantities (AB, BC, CA) in conjunction with positive-sequence memory voltage [6]. For simplicity, we assume all fault loops are balanced for this fault type, and therefore, (10) is equivalent to a traditional distance element implementation for three-phase faults.

$$T21P = RE\left[SOP \bullet SPOL^{*}\right] \tag{10}$$

where:

$SOP = I1_{REPLICA} \bullet |Z1_{Reach}| - V1$ (forward-reaching zone)

$SOP = -I1_{REPLICA} \bullet |Z1_{Reach}| - V1$ (reverse-reaching zone)

$SPOL = V1_{MEM}$

When T21P evaluates to a value greater than zero, the distance element operates. This occurs when the operating signal (SOP) is less than 90 degrees from the polarizing signal (SPOL). When T21P evaluates to a value less than or equal to zero, the distance element restrains. This occurs when the SOP is 90 degrees or more from SPOL. We include SOP for a reverse-reaching distance element (R1 in our example) and a forward-reaching distance element (R2 in our example).

Fig. 6 showcases (10) in action and offers a phasor diagram plot of the quantities SOP (named SOPR1 and SOPR2), SPOL (named $V1_{MEM}$), and V1 (named V1R1 and V1R2) for R1 and R2. To illustrate, R1 has a reverse reach equal to ZL1 and R2 has a forward reach set equal to 2 • ZL1. In practice, the reverse-reaching Zone 3 of Relay 1 must overreach, with margin, the forward-reaching Zone 2 of Relay 2 for faults behind Relay 1 [7].

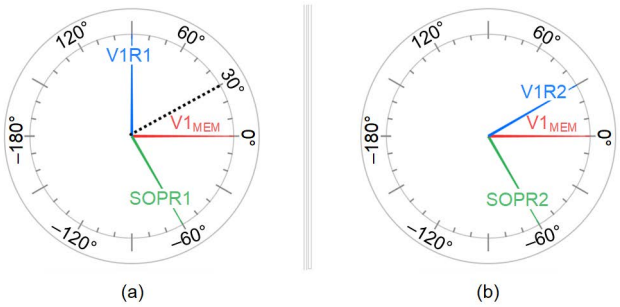

Fig. 6. Distance Element Evaluation for R1 Zone 3 (a) and R2 Zone 2 (b) During the Example Three-Phase Cross-Connect Fault

R1 sees the fault within its pilot blocking zone of protection and operates since the angle difference between SOPR1 and $V1_{MEM}$ is 60 degrees. However, once $V1_{MEM}$ travels +30 degrees, the distance element drops out. This happens after about 50 ms, as shown in Fig. 4.

R2 also initially sees the fault within its pilot tripping zone of protection. The R2 distance element is right at the "no operation point" once the memory component of $V1_{MEM}$ is expired (V1R2 and SOPR2 are 90 degrees apart). It takes over 300 ms for memory to expire based on the memory decay shown in Fig. 4.

Assuming each relay implements the same memory time constant, R1's reverse-reaching zone drops out well before R2's forward-reaching zone drops out. In a DCB scheme, this means that R2 issues a trip for this fault, which relates exactly to the case study presented in this paper.

In fact, many relays are at risk of misoperation throughout the system for this type of fault. Equations (11) and (12) show the minimum reach requirements to have the R1 reverse zone and the R2 forward zone operate for a three-phase series fault. (The appendix offers the derivations.)

$$ZR1_{Reach} = \frac{ZS1 - \frac{ZL1 + ZR1}{2}}{1.5} \quad (11)$$

$$ZR2_{Reach} = \frac{ZS1 + ZL1 - \frac{ZR1}{2}}{1.5} \quad (12)$$

In the simple example system in which ZS1 = ZR1 = ZL1, the minimum required reach for R1 to operate is 0 ohms. This means that regardless of the reach set, a reverse-looking distance element operates. A similar condition can develop for forward-looking distance elements at R2. For example, if ZS1 = ZL1 and ZR1 = 4 • ZL1 and we insert that into (12), the minimum reach required for R2 to operate is 0 ohms. In these system conditions, a Zone 1 instantaneous distance element at R2 operates regardless of the set reach. This points out that while a communications-assisted trip scheme restrains while memory is available due to information shared between terminals, instantaneous underreaching elements pose a security risk depending on the system.

III. Event Analysis, Solutions, and Advancements in Distance Element Polarization

In this section, we analyze the key events from the relays on Line 1 and Line 2. We review enhancements to traditional protection to detect this fault type. We then discuss recent advancements in transmission line relays that improve the security of elements that utilize positive-sequence memory polarization.

A. Line Current Differential Relays (Line 1)

Line 1 is protected by an 87L element. Fig. 7 shows the phasors for this fault from each terminal, where IpL currents are from Relay 3 and IpX currents are from Relay 4 (p = A, B, or C). The phasor magnitudes are equal at each end of the line (9,400 A). ICL is 180 degrees from IAX, IAL is 180 degrees from IBX, and IBL is 180 degrees from ICX. This shows that a series fault occurred and the phasing at Relay 3 is CAB, while the phasing at Relay 4 is ABC.

The 87L relay adds IAL and IAX and sees over 16,000 A of differential current. This is the differential current on Phases B and C as well. This exceeds the pickup value of 1,200 A set in the relay, and thus, it operates fast, tripping Breakers A and B.

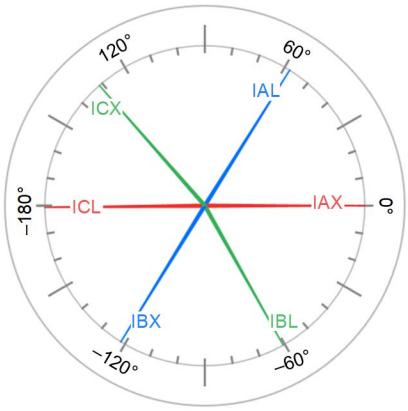

Fig. 7. Line 1 Current Differential Phasor Diagram for the Actual Three-Phase Cross-Connect Fault

B. Relay 4, Zone 1 Operation (Line 1)

Although Breaker A and Breaker B were opened by the 87L scheme, the underreaching Zone 1 element in Relay 4 is also called to trip Breaker B. While the breaker that closed (Breaker A) is outside of the Zone 1 reach of Relay 4, the large shift in V1 voltage increases the likelihood of a Zone 1 trip. The phasors for V1, $V1_{MEM}$, and SOP at fault initiation are shown in Fig. 8, as well as the Zone 1 digital signal assertion (Z1).

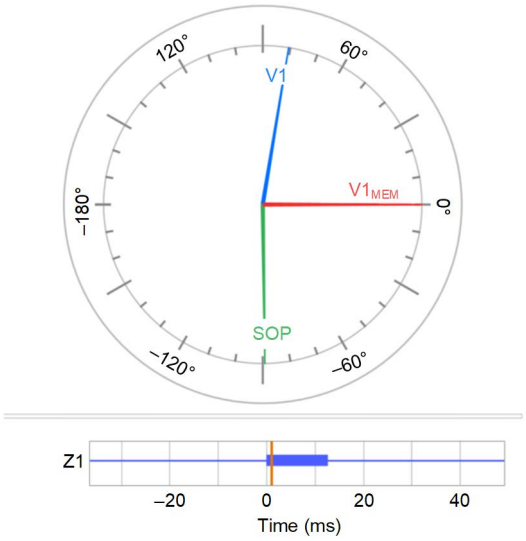

Fig. 8. Relay 4 Phasors for the Actual Three-Phase Cross-Connect Fault

The Z1 assertion occurs near fault initiation and is short in duration. The phasor SOP is within 90 degrees of $V1_{MEM}$ for approximately 10 ms while $V1_{MEM}$ is still close to $V1_{PRE}$. However, as the memory component of $V1_{MEM}$ decays to the point at which $V1_{MEM}$ is more than 90 degrees from SOP, Z1 deasserts.

C. DCB Scheme (Line 2)

Line 2 is protected with a DCB scheme. First, we discuss the event starting at Relay 2, which sees this fault in the forward direction.

1) Relay 2

The oscillography for this three-phase cross-connect fault is shown in Fig. 9 where Relay 2 asserts a pilot tripping element (Z2). The digital signal IN1 is the blocking signal received from Relay 1 (the remote relay). Initially, Relay 2 is prevented from tripping on the DCB scheme by the receipt of the blocking signal from Relay 1. However, just over 50 ms from fault initiation, IN1 drops out and Relay 2 trips on the DCB scheme, indicated by OUT1 in Fig. 9.

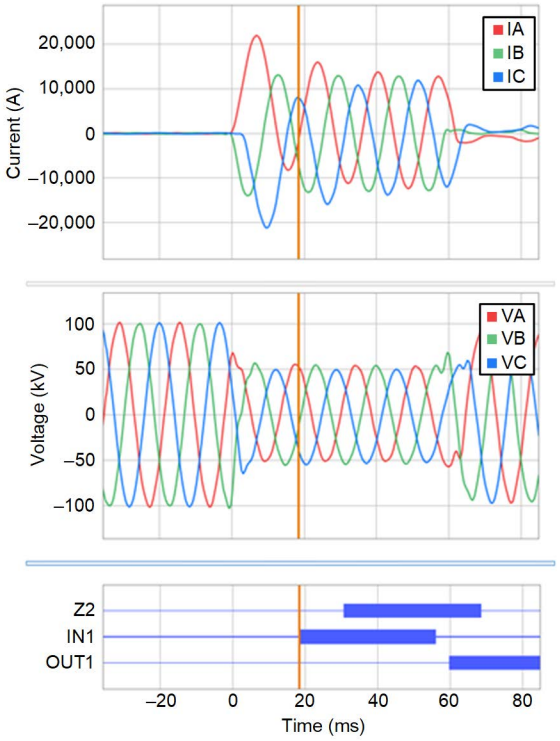

Fig. 9. Relay 2 Oscillography for the Actual Three-Phase Cross-Connect Fault

Fig. 10 shows the phasor view of V1, $V1_{MEM}$, and SOP from Relay 2 at fault initiation. V1 and SOP are less than 90 degrees apart, so even once memory expires, Relay 2 still maintains a pilot tripping element (Z2) assertion. The following phasor plot is similar to the phasor plot provided in Fig. 6 for R2 in Section II.C.

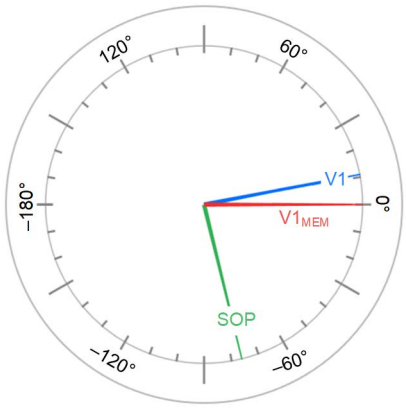

Fig. 10. Relay 2 Phasors for the Actual Three-Phase Cross-Connect Fault

2) Relay 1

The Relay 1 oscillography for this fault is shown in Fig. 11. The relay initially asserts the reverse-looking pilot blocking bit (Z3), but just under 50 ms from fault initiation, Z3 drops out while the fault is still present.

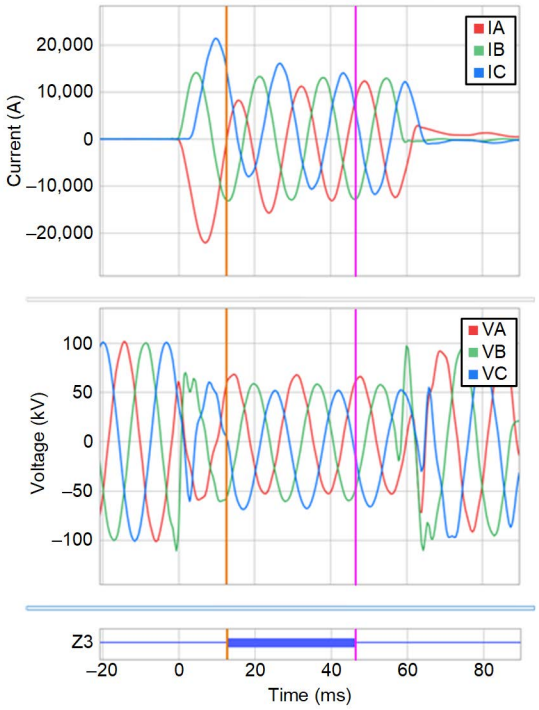

Fig. 11. Relay 1 Oscillography for the Actual Three-Phase Cross-Connect Fault

Fig. 12 shows the phasor view of V1, $V1_{MEM}$, and SOP from Relay 1 at fault initiation. $V1_{MEM}$ and SOP are less than 90 degrees apart, so initially, the relay asserts Z3, as seen in Fig. 11. However, once the memory component of $V1_{MEM}$ begins to expire, eventually Z3 drops out as $V1_{MEM}$ is more than 90 degrees from SOP. This occurs when $V1_{MEM}$ has shifted +30 degrees from $V1_{PRE}$. The following phasor plot is similar to the phasor plot provided in Fig. 6 for R1 in Section II.C.

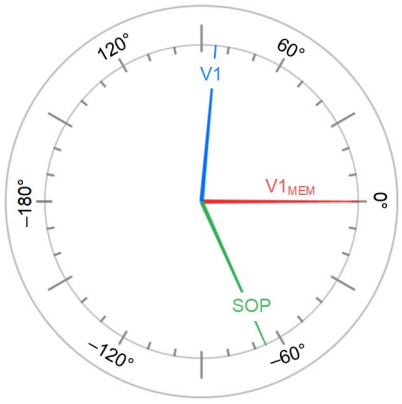

Fig. 12. Relay 1 Phasors for the Actual Three-Phase Cross-Connect Fault

D. Solutions and Advancements

In this section, we discuss solutions to dependability and security for three-phase cross-connect faults, including SOTF settings and advancements in memory voltage algorithms.

1) Line Current Differential and SOTF

During a three-phase cross-connect condition, communication-scheme security is at risk, especially the longer the fault remains. As such, quick and dependable operation of primary protection can prevent adjacent communication-scheme protection misoperations related to a three-phase cross-connect condition.

87L offers selective, dependable, and relatively fast clearing for this fault. However, if 87L is not present, the next best selective form of protection for closing into a cross-connect fault is SOTF protection. Since this is a series fault, only one breaker must open to isolate the condition, and ideally it is the breaker that closed, creating the series fault.

Reference [8] discusses the reliability and performance of instantaneous phase overcurrent (50P), undervoltage supervision of instantaneous phase overcurrent element (50P AND 27P), overreaching positive-sequence memory-polarized Zone 2 (Z2), and nondirectional distance protection (21ND). In the following discussion, refer to Relay R1 in Fig. 2. There are a few challenges when relying on SOTF to clear this type of fault:

- Enabling SOTF reset disables SOTF protection when healthy voltage is seen by the PTs. This prevents SOTF at Breaker 1 from enabling when Breaker 2 is closed, energizing the line PTs at Breaker 1. For SOTF to be available for cross-connect faults, SOTF reset for healthy voltage must be disabled.
- Undervoltage supervision must be set above 0.50 pu of the system nominal voltage if using 50P AND 27P logic. During a three-phase cross-connect condition, the voltage magnitude does not collapse to zero as it does for a close-in three-phase bolted fault. A relay located at the midpoint of the system in Fig. 2 measures the lowest voltage magnitude, and this is 0.50 pu of the system nominal voltage, as per the discussion in Section II.B. This is equivalent to the minimum phase voltage measured for a two-phase cross-connect condition [1].
- The 50P setting needs to be set using (1), with margin. Depending on the system, this may require a lower setting than what is recommended in [8].
- The Z2 element at Relay R1 does not operate as the fault appears reverse (see the phasors from Fig. 5).
- The 21ND element at Relay R1 may operate depending on the system but is not more dependable than 50P AND 27P logic.

2) Longer Memory Voltage

In the analysis in Section III.C.2, the R1 Zone 3 (Z3) element dropped out due to the decay of the memory component of the polarizing voltage. Fig. 13 shows the results of playing the event into a relay that was released in 2020 with a more robust V1 memory polarization algorithm ($V1_{MEM.NEW}$) compared to the 1993 vintage relay in service at the time of the fault ($V1_{MEM.OLD}$). The $V1_{MEM}$ traces in Fig. 13 show the angular difference between $V1_{MEM}$ and $V1_{PRE}$ for the duration of the fault. The 30DEG threshold shows when the angular difference between $V1_{MEM}$ and $V1_{PRE}$ is 30 degrees and is used to mark the phase angle difference for which the Zone 3 element drops out. The digital signal 52A_BKA deasserts when the 87L relay on Line 1 opens Breaker A, thus removing the cross-connect fault.

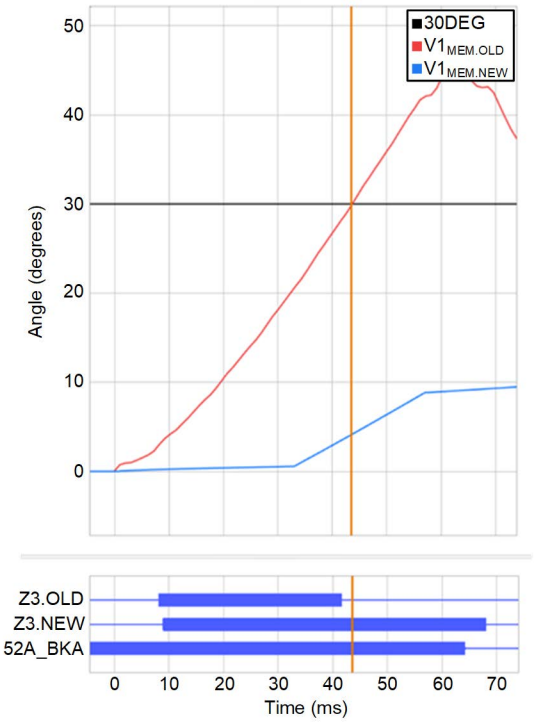

Fig. 13. 1993 Vintage Relay and 2020 Vintage Relay $V1_{MEM}$ Comparison

The $V1_{MEM.OLD}$ and $V1_{MEM.NEW}$ traces in Fig. 13 show the memory voltage performance during this fault. The 2020 vintage relay memory voltage component of the polarizing signal decays much more slowly compared to the 1993 vintage relay, and it never exceeds 10 degrees, which allows Z3.NEW to remain asserted throughout the duration of the fault. The 1993 vintage relay polarizing signal uses a short time constant for the memory component of the polarizing signal since the V1 voltage magnitude is much larger than 10 percent of the system nominal voltage (not shown, but equal to about 0.57 pu of the system nominal voltage). This makes $V1_{MEM.OLD}$ deviate from the pre-fault voltage quickly. In under 50 ms from fault initiation, the Z3.OLD element has dropped out.

The 2020 vintage relay uses a phase-locked loop control system that generates an output signal (V1POL) based on the input voltage (V1) and the measured system frequency [9]. Additionally, the relay implements various modes of distance element polarization that allow for adaptability to various system conditions to maintain relay reliability. For example, if an unstable power swing is detected, the relay utilizes a self-polarization mode rather than a memory polarization mode to maintain security. Further, when the memory voltage polarization mode is used, another security measure is to limit memory action to 300 ms to mitigate issues caused by fast frequency excursions. However, if a zero-voltage three-phase fault remains longer than 300 ms, the relay switches to a current polarization mode to maintain dependability and security of distance elements for up to 2 seconds. This level of distance element polarization control in conjunction with a finite memory voltage time limit allows a slow-decaying memory voltage component to be used securely.

IV. 87R Operation for a Three-Phase Cross-Connect Fault

In this section, we shift our focus from the line protection to the transformer protection. Relay 5, which is protecting the loaded 15 MVA, 120/13.8 kV DABY step-down transformer, located at Breaker E in Fig. 1, was the last relay to trip for this series fault. Fig. 14 narrows the focus area down from the original single-line diagram shown in Fig. 1 and focuses on the transformer configuration for this section. For a review of transformer differential protection, please refer to [10], [11], and [12].

The TAP settings and angle compensation settings were applied appropriately on Relay 5 for the DABY transformer-connected nonstandard phase-to-bushing connections, as seen in Fig. 14. For more background on compensating for nonstandard phase-to-bushing connections, refer to [11].

The DABY transformer is protected by an 87R element that utilizes harmonic restraint to keep the element secure during transformer energization.

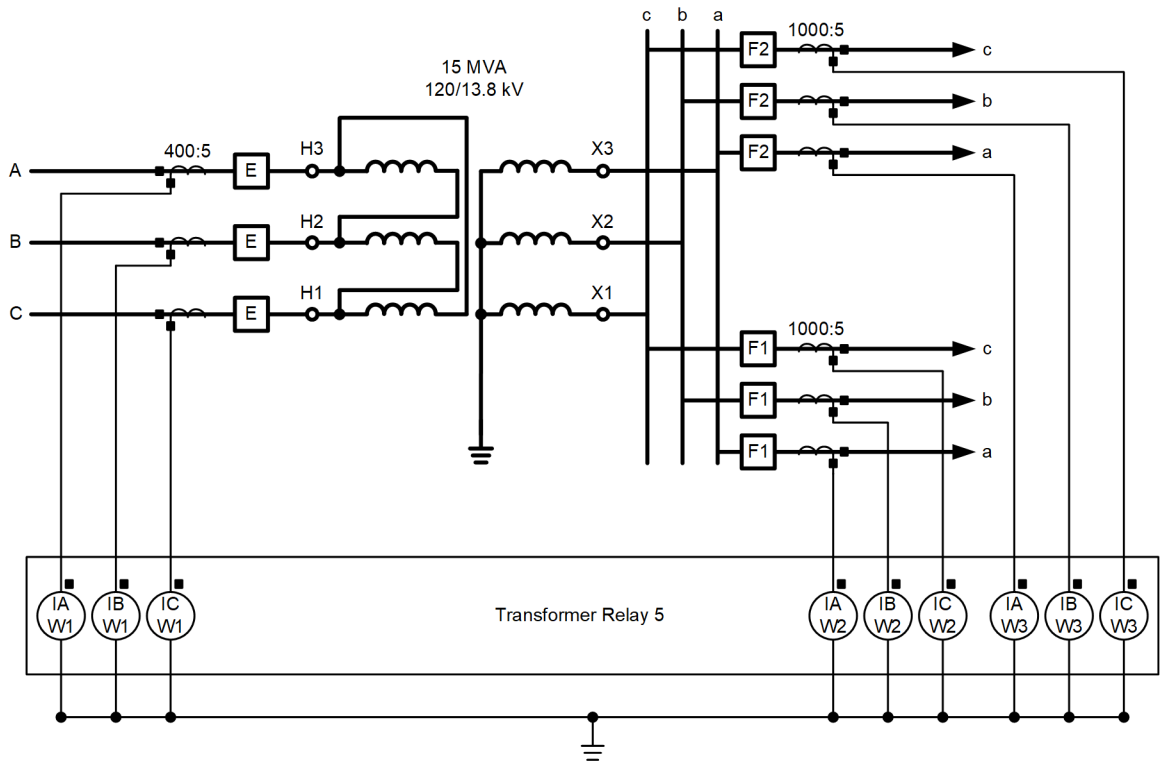

Fig. 14. Three-Line Diagram of DABY Transformer Configuration

A. *Overview of the Transformer Event*

Fig. 15 shows the event report captured by the transformer relay during the fault. The event captured can be segregated into two parts.

Just before Breaker A closes into the three-phase cross-connect fault, the transformer is fed from Breaker D (shown by assertion of 52A_BKD) and the load is being fed by the transformer. Part 1 in Fig. 15 is roughly 66 ms long and begins when the ABC to CAB cross-connect fault at Breaker A was imposed on the system (shown by assertion of 52A_BKA). During Part 1, both Source 1 and Source 2 are supplying the transformer and its load. Fig. 15 shows the raw compensated currents, in per unit of full-load amperes, for Phase A, B, and C CTs making up the zone of 87R protection for the transformer. W1A, W1B, and W1C are the raw compensated currents on the delta side of the transformer. W2A, W2B, and W2C are the raw compensated currents on the wye side of the transformer located at Breaker F1. W3A, W3B, and W3C are the raw compensated currents on the wye side of the transformer located at Breaker F2. The raw voltage signals from the 120 kV side of the transformer for Phases A, B and C are also captured in Fig. 15 (VA, VB, VC). Near the end of Part 1, Relay 5 trips on 87R assertion (via Phase C) just before Part 2 begins.

Part 2 in Fig. 15 begins the moment Breaker A opens (52A_BKA deasserts) and the transformer is again fed from Source 2 only. Part 2 ends when Breaker D has opened (52A_BKD deasserts) based on the DCB discussion and analysis in Section III and the transformer is officially isolated from each voltage source.

Breaker E opens (52A_BKE deasserts), but it is after the transformer is already isolated by the opening of Breakers A and D.

From Fig. 15, it is clear that the transformer experiences classic magnetizing inrush current, which is seen on all the currents entering and leaving the transformer. The subject transformer draws inrush current, and so does any downstream distribution transformer connected to the 13.8 kV winding. Transformer inrush is a well-documented phenomenon that occurs when a transformer is initially energized [13] [14] [15]. However, once the core of the transformer is magnetized and load is applied, magnetizing inrush is typically not seen with conventional shunt type faults. However, the event described in this paper is not a shunt fault but a three-phase series fault. So, to better understand why there is magnetizing inrush current for this event on a loaded transformer, it is important to understand the behavior of the voltages relative to the transformer's core flux.

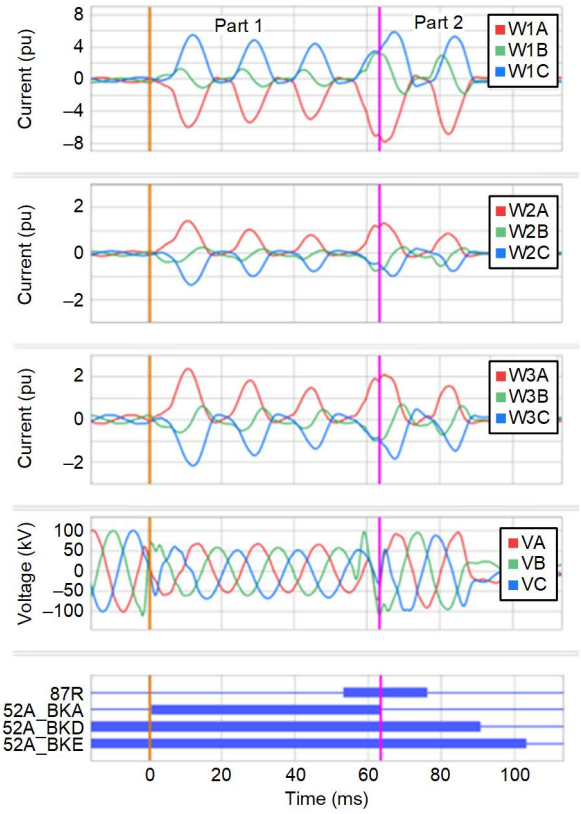

Fig. 15. Phase A, B, and C Raw Compensated Current and Voltage Measurements for the Actual Three-Phase Cross-Connect Fault

B. *Voltage and Flux Relationship to Explain Inrush Current for a Cross-Connect Series Fault*

During a three-phase cross-connect condition, a transformer draws significant inrush current due to the sudden change of voltage in conjunction with the high amount of flux present in the magnetic core of the transformer. During typical transformer inrush, there is initially no voltage applied to the transformer but there may be some remnant flux (Ψ_R) present in the transformer magnetic core. When a switch is closed to energize the transformer, a nominal voltage is applied to the transformer and flux (Ψ) generated from the applied voltage either adds or subtracts from the magnetic core's remnant flux. As the flux required to sustain the applied voltage becomes large, the magnetic core may saturate, leading to inrush current.

The same mechanism occurs for a three-phase cross-connection, with the exception that the remnant flux is replaced with the flux present just before the cross-connect fault (Ψ_i) and the flux (Ψ) generated from the newly applied voltage adds or subtracts to this initial value.

Disregarding the turns of the transformer for simplicity, the flux of a time-varying signal can be defined, as shown in (13).

$$\psi = \int v(t)dt + \psi_i \tag{13}$$

where:

v is a time-varying voltage signal.

Ψ is a time-varying flux signal measured in webers (Wb).

Ψ_i is the flux present just before the switch closes.

Assuming that the voltage is defined by the cosine function in (14), this then creates the following relationship from (13), where the integral of (15) results in (16).

$$v = \cos(\theta) \tag{14}$$

$$\psi = \int \cos(\theta)d\theta + \psi_i \tag{15}$$

$$\psi = \sin(\theta) + \psi_i \tag{16}$$

where:

θ is the angle of the signal.

Equation (16) shows the flux defined as the sine function, which shows that the flux lags the applied voltage by 90 degrees.

The material used in the magnetic core of the transformer limits the amount of flux available. To model this simply (see Fig. 16), consider a single-phase transformer magnetic core connected to one of two separate voltage sources via a switch (SW). V_{NOM} represents the voltage applied to the transformer prior to the cross-connect fault. V_{FAULT} represents the voltage applied to the transformer when the cross-connect fault occurs. The magnetic core (Ze) can be treated as a flux limit switch (FLSW) in series with an inductance (L), which we refer to as the excitation branch.

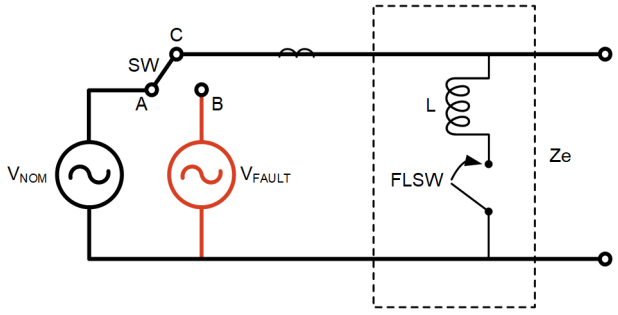

Fig. 16. Simplified Transformer Circuit

Prior to the fault, SW is in Position A for a long time and the FLSW is open. When the fault occurs, SW changes from Position A to Position B and the flux present at the time of the switch transition is retained. If the flux required to sustain the newly applied voltage is within the flux limit, FLSW is open (Ze = ∞). If the flux required to sustain the newly applied voltage is greater than the flux limit, the FLSW is closed (Ze = L).

Fig. 17 shows the Ψ – Ie curve that creates the excitation branch (Ze) shown in Fig. 16. Ie represents the excitation current consumed by the excitation branch. The vertical line of the Ψ – Ie curve represents an excitation branch apparent impedance of Ze = ∞ (FLSW open). Under this condition, no excitation current is consumed by the excitation branch. When the flux limit is reached, Ze = L (FLSW closed). Under this condition, the excitation current consumed by the excitation branch is limited by L. We selected the flux limit to be equal to the nominal voltage, so that FLSW remains open when nominal voltage is applied.

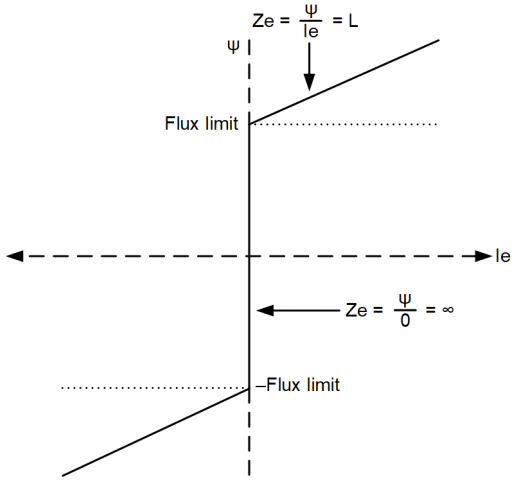

Fig. 17. Simplified Ψ – Ie Curve

Fig. 17 is like a B-H curve but ignores the area of the magnetic material within the transformer core for the sake of simplicity. For a more detailed discussion on B-H curves and transformer inrush, see [14].

To put the principle explained in this subsection into practice and to demonstrate the existence of inrush and the extent to which it exists during a three-phase cross-connect condition, consider an example for one of the phases. The captured voltage and differential operate current for Phase C, which is the phase that caused the 87R operation, are shown in Fig. 18. IOPC represents the Phase C inrush current drawn by the subject transformer.

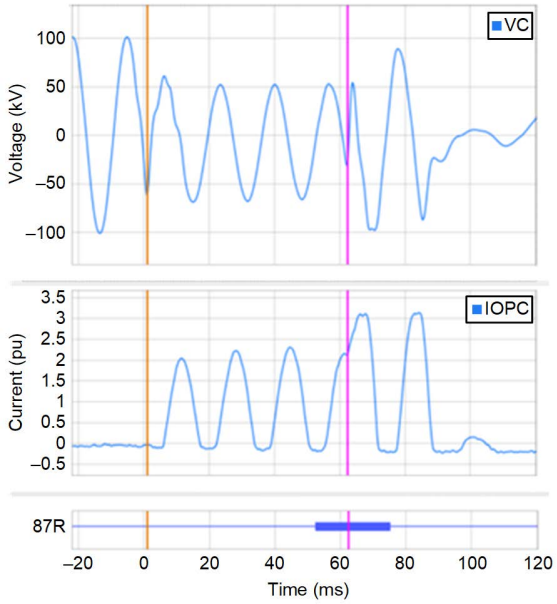

Fig. 18. Phase C Captured Voltage and Operate Current for the Actual Three-Phase Cross-Connect Fault

The Phase C voltage (top trace in Fig. 18) shows an abrupt change in voltage just before a negative voltage peak (indicated by the orange cursor). The voltage shifts +90 degrees, and the voltage magnitude drops to approximately 0.57 pu, which is discussed in Section II, as the transformer is located very close to Relay 1. After 60 ms and just past a positive-to-negative zero crossing, the voltage on Phase C returns to normal, shifts –90 degrees, and returns to 1 pu.

These exact conditions were simulated using (14), (16), the circuit from Fig. 16, and the Ψ – Ie curve from Fig. 17. The results are shown in Fig. 19.

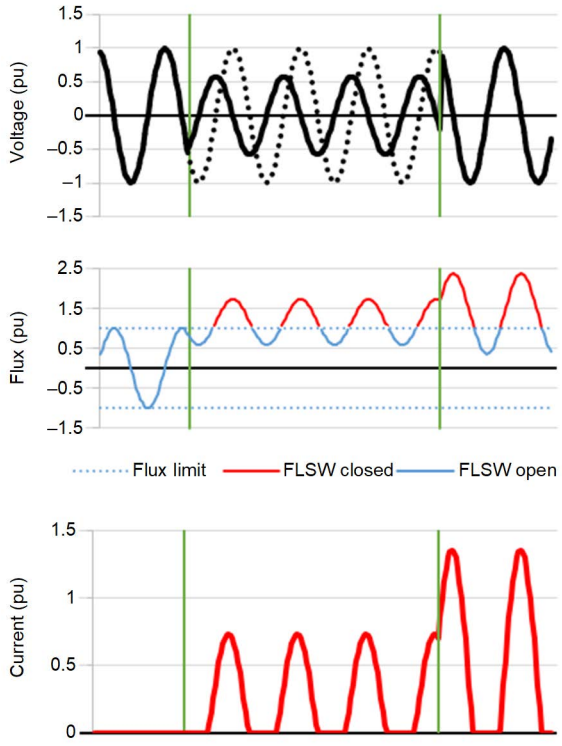

Fig. 19. Voltage (Top), Flux (Middle), and Inrush Current (Bottom) for the Example Three-Phase Cross-Connect Fault for Phase C Only

The top plot in Fig. 19 shows the applied voltage for a cross-connect fault (solid trace) and the voltage signal if no cross-connect fault had occurred (dotted trace). Vertical cursors are placed at the two key moments of the event: when the cross-connect fault initially occurred and when the cross-connect fault was cleared. The voltage trace matches closely with the actual voltage seen in Fig. 18.

The middle plot shows the flux and the flux limit at which FLSW operates. When the flux is below the upper flux limit, FLSW is open and the flux trace is blue. When the flux is above the flux limit, FLSW is closed and the flux trace is red.

The bottom plot shows the excitation current drawn by the transformer core. The excitation current is drawn when FLSW closes.

The Fig. 19 current follows the actual inrush current waveform shape seen in Fig. 18 very closely. Seeing the flux present in the magnetic core helps identify why inrush occurs during this cross-connect condition.

When Phase C voltage makes a positive-to-negative zero crossing just before the leftmost green cursor, the flux is near positive peak value. When the voltage is abruptly shifted +90 degrees, the newly applied fault voltage begins to rise before reaching the negative peak value of the pre-fault voltage. Since the flux lags the voltage by 90 degrees, the flux does not rise immediately (it falls some), but it eventually does rise past the flux limit. This leads to excitation current, as shown in Fig. 19.

When the cross-connect fault is cleared (indicated by the rightmost green cursor), the magnetic core is already consuming Ie. The –90-degree shift in voltage near the positive-to-negative zero crossing leads to an abrupt rise in voltage, and this drives the flux even higher, which leads to even more Ie.

The simplified model in Fig. 16 is a single-phase transformer with a switch in series with an inductor representing a magnetic core, while the transformer in service during this event is a three-phase transformer with a true magnetic core. Flux interaction within a three-phase transformer is more complex than in a single-phase transformer [14], and true B-H curves provide different inrush waveshapes. There are many classical publications that use slightly different B-H curves to illustrate inrush current [16] [17]. We offer a simplified model in this paper to describe the concepts.

This subsection highlights the fact that transformer inrush current is possible for cross-connect faults. The theoretical approach offered in this subsection also explains why there is inrush current when the cross-connection is removed by the opening of Breakers A and B.

Furthermore, inrush current can be even more extreme for cross-connect faults compared to when a transformer is initially energized. This overall concept can be compared to a breaker restrike condition when de-energizing a transformer. Reference [14] shows that during this type of condition, the transformer magnetic core can go into deep saturation, which generates high inrush current and potentially low second-harmonic content. More information on inrush and unique saturation phenomena can be found in [18] and [19].

C. Why Did 87R Assert With Harmonic Restraint Enabled?

Transformer relays are equipped with multiple techniques, such as harmonic restraint and harmonic blocking, to allow the 87R element to remain secure during inrush conditions. Each technique has dependability and security considerations, which can be found in [15]. At the time of the event, harmonic restraint was enabled on the transformer differential relay.

Equation (17) describes the basic operation condition for a percentage-restraint differential relay. The operate current (IOPp) must exceed the minimum operate current (O87P) or a percentage (SLP) of the restraining current (IRTp), whichever is greater. This is done on a per-phase basis (where p in IOPp and IRTp stand for Phase A, B, or C). IOPp is the magnitude of the vectoral sum of all compensated currents in the zone of protection, while IRTp is the sum of all the current magnitudes in the zone of protection multiplied by 0.5.

$$\mathrm{IOPp} > \max\left[\mathrm{O87P}, \left(\frac{\mathrm{SLP}}{100} \bullet \mathrm{IRTp}\right)\right] \qquad (17)$$

Enabling harmonic restraint for inrush security alters (17) by adding second- and fourth-harmonic content in the restraint signal, as shown in (18) and (19).

$$\text{IOPp} > (\text{HR\_THRESH\_p}) \tag{18}$$

where:

$$\text{HR\_THRESH\_p} = \max\left(\text{O87P}, \frac{\text{SLP}}{100} \bullet \text{IRTp} + k_2 \bullet \text{IOPp}_{2H} + k_4 \bullet \text{IOPp}_{4H}\right) \tag{19}$$

where:

k_2 is a scaling constant for the second harmonic.

IOPp_{2H} is the second-harmonic content of IOPp in per unit.

k_4 is a scaling constant for the fourth harmonic.

IOPp_{4H} is the fourth-harmonic content of IOPp in per unit.

By adding a scaled value of second and fourth harmonics to the restraining signal, the relay security is improved as more operate current is required to overcome the restraining signal during inrush, which is typically rich in even harmonics. Relay 5 had harmonic restraint enabled with the scaling constant k_2 set to 100/15, which equals 6.67 per unit. For the case study, k_4 can be neglected and assumed to be negligible.

According to (18) and (19), for the 87R element to assert, the operate current (IOPp) must be greater than the HR_THRESH_p threshold for Phase A, B, or C. In Fig. 20, the IOPC per-unit current is above the HR_THRESH_C threshold and 87R asserts after a short security delay.

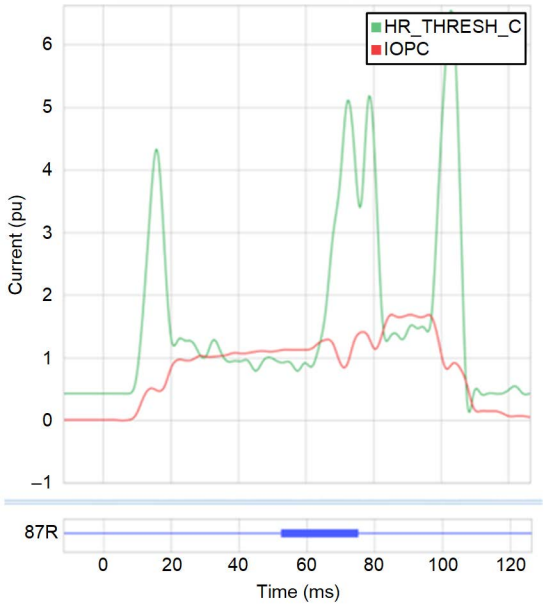

Fig. 20. IOPC Compared to HR_THRESH_C for the In-Service Transformer Differential Relay

Because of the nature of the fault, the inrush current has low levels of the second-harmonic component, IOPp_{2H}, in (19). So, the overall boost that IOPp_{2H} provides to the restraint quantity, defined as HR_THRESH_p in (19), is minimal.

It is evident in this section that harmonic restraint was not adequate to restrain the 87R element from operating for the fault exhibited in this paper. As mentioned in this section, harmonic-based algorithms are well-known and used in the industry for security during inrush conditions. Altering the harmonic restraint setting, k_2, or enabling harmonic blocking may have prevented an 87R operation for the fault shown in this paper, but doing so would not be without limitations [15].

D. 87R Security Advancements in Microprocessor-Based Transformer Relays

For inrush current with a low second harmonic in a loaded transformer, there are two advancements in modern differential relays that can help provide 87R security:

- The waveshape-based inrush technique, which detects transformer inrush by identifying flat spots in the differential current waveform shape. This information is used to restrain the relay [14] [20].
- An adaptive slope, which uses external fault detection (EFD) logic to bias the percentage-restraint characteristic toward security for external faults [21] [22]. This logic engages a higher slope setting when a sudden change of restraint current is detected with no corresponding change in operate current for a short amount of time (typically less than 0.1 cycles) after fault initiation. This indicates an external fault has occurred, and the relay adapts to a more secure slope setting. As time progresses, the CT may begin to saturate and produce false operate current for the external fault. By using a more secure slope, the relay is more secure against CT saturation throughout the full duration of the external fault.

Fig. 21 shows the event played back in a modern transformer differential relay with an adaptive slope and waveshape-based inrush detection available. The external fault detector asserts the CONC digital signal, which indicates that the relay switched to high-security mode. If we compare Fig. 20 to Fig. 21, it is clear that switching to high-security mode raises the HR_THRESH_C signal, which adds security. In Fig. 21, there are two 87R digital signals: 87R_WS_OFF and 87R_WS_ON. When waveshape blocking is turned off, the 87R still asserts when the cross-connect fault is cleared (indicated by the assertion of 87R_WS_OFF after a short security delay). Recall from Fig. 19 that when the cross-connect is cleared, the transformer goes further into core saturation, which reduces the amount of available second-harmonic content that can be used to restrain the relay. Fig. 21 shows the digital signal 87WBC, which indicates that waveshape blocking is engaged for Phase C. 87WBC asserts early in the event, thus indicating that waveshape blocking is enabled and ensuring security for the 87R element for inrush conditions, even for inrush cases with low second-harmonic current.

Fig. 21 shows that, with waveshape blocking turned on, the 87R element remains secure (indicated by a nonassertion of 87R_WS_ON).

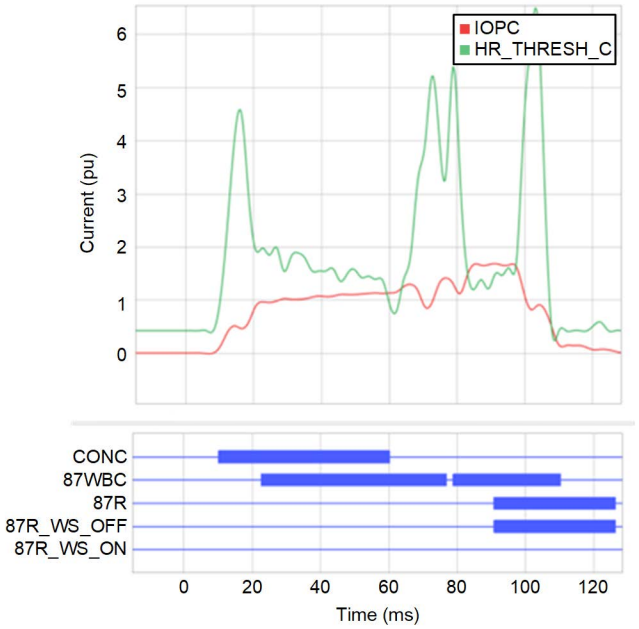

Fig. 21. IOPC Compared to HR_THRESH_C From the Field Event Played Back Into a Modern Transformer Differential Relay

The assertion of CONC occurs when there is a change in restraint current (DIRT_C) that exceeds a pickup of 1.2 pu but the change in operate current (DIOP_C) does not exceed a pickup of 1.2 pu. This comparison is run through a short pickup timer, which is typically set less than 0.1 cycles. Fig. 22 shows the DIOP_C and DIRT_C signals for Phase C.

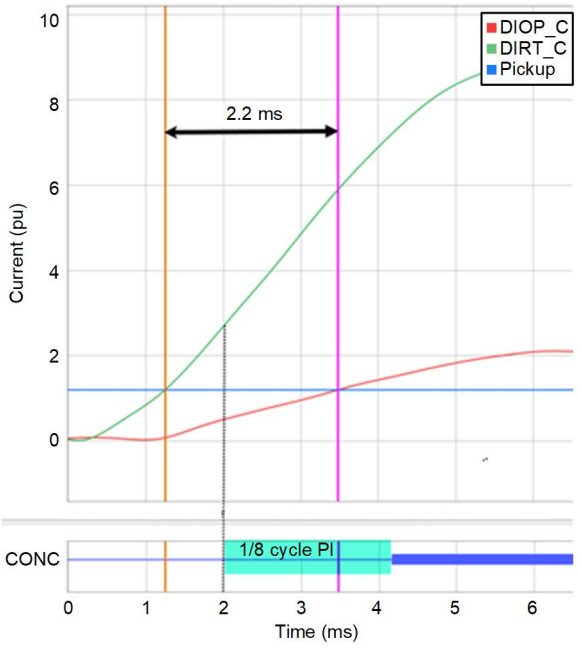

Fig. 22. DIOP_C and DIRT_C for the Field Event Played Back Into a Modern Transformer Differential Relay

In traditional inrush cases, the transformer is not connected to the load and the transformer is initially de-energized. When the breaker that applies voltage to the transformer is closed, the only current visible to the differential relay is the excitation current drawn by the magnetic core of the transformer. This means that DIOP and DIRT change at the same time, and the relay does not move to Slope 2.

In this event, the transformer is already energized with the load connected prior to the change in voltage that led to the magnetic core consuming more excitation current. DIRT_C increases immediately, while DIOP_C increases with a short delay in time, as shown in Fig. 22. This is because the sudden change in voltage immediately changed the current consumption of the connected loads. Since these loads are external to the zone of protection, this change in current does not produce operate current, but it does change the restraint current. The increase in excitation current, which produces operate current, does not happen immediately. After DIRT_C increases above the threshold, it takes 2.2 ms for the DIOP_C value to increase above the threshold. This can also be seen in Fig. 19 as the flux takes some time to exceed the upper flux limit, leading to the core drawing inrush current. In effect, the principle of delayed CT saturation to detect external faults also provides security for delayed increases in excitation current.

However, when the cross-connect condition is removed, the external fault detector does not assert because DIOP_C and DIRT_C cross the threshold only 1.1 ms apart from each other (not shown). This short delay between when DIOP_C and DIRT_C cross the threshold occurs since the transformer core is already operating in the low slope region of the B-H curve and any further changes in voltage will lead to an immediate change in operate current. In this event, the EFD provides security for the initial cross-connect, but not when the cross-connect fault is removed.

To summarize, the EFD adds security to transformer differential relays for external faults and cases in which a loaded transformer draws excitation current due to a significant change in voltage. Waveshape blocking provides security for inrush events in which there is low second-harmonic current. The two algorithms together provide excellent security for three-phase cross-connect faults such as the one analyzed in this paper.

V. Conclusion

A three-phase cross-connect fault is not a traditional fault type and can challenge relay security at various locations of the power system. This is a man-made series fault, typically created by incorrect phasing on each side of a breaker before it is subsequently closed. This type of fault can produce very high fault current. Since this is a series fault, only one breaker must open on the system to interrupt the fault current, and ideally, it is the breaker that initially closes to create the condition so that selectivity is maintained.

Transmission line relays, which rely on positive-sequence memory polarization for directional elements and distance elements, may misoperate for this fault type. Zone 1 elements on adjacent lines may operate due to the large shift in voltage that occurs. These operations are unavoidable. Communications-assisted tripping schemes on adjacent lines,

especially DCB schemes, are also suspectable to misoperation. Initially, positive-sequence memory voltage maintains security, but as the memory component of the polarizing signal decays, directionality is lost and relays at each end of the line may no longer agree that the fault is external. Recent relay advancements in memory polarization provide additional security for this fault type.

The SOTF logic can trip for the initial breaker closing if SOTF is enabled when voltage is applied to the line PTs. Further, the SOTF logic that utilizes undervoltage supervision should have 27P set above 50 percent nominal voltage to be active for three-phase cross-connects, discussed in this paper, and two-phase cross-connects, discussed in [1].

Transformer differential relays may see inrush current that contains little second-harmonic content during a three-phase cross-connect condition. The large change in voltage, particularly the abrupt change in the phase angle, leads to inrush current. When the cross-connect fault is cleared by remote relays, a second change in voltage occurs that may lead to a further reduction in the second-harmonic content of the inrush current. Recent advancements in transformer differential relay protection improve security for this fault type by utilizing EFD and waveshape-inrush blocking algorithms.

Modern digital relays use new components that offer better analog-to-digital conversion, faster microprocessors, and more memory storage, just to name a few. This increase in available horsepower has allowed relay designers to improve the reliability and performance of digital relays by implementing algorithms that have not been possible in the past. This paper highlights an example of how these new algorithms provide additional relay security for an unusual fault type.

VI. Appendix

A. Three-Phase Cross-Connect Basic Formulas

In (20), we show the formulas that define the positive-sequence voltage, positive-sequence current, and positive-sequence replica current for a three-phase cross-connect fault.

$$\begin{aligned}
&V1R1 = \left(\frac{X+(1+Y)\angle 120}{X+1+Y}\right), V1R2 = \left(\frac{X+1+Y\angle 120}{X+1+Y}\right)\\
&I1R1 = -\left(\frac{\sqrt{3}\angle -30}{(X+1+Y)\angle 90}\right), I1R2 = \left(\frac{\sqrt{3}\angle -30}{(X+1+Y)\angle 90}\right)\\
&I1R1_{Replica} = -\left(\frac{\sqrt{3}\angle -30}{(X+1+Y)}\right), I1R2_{Replica} = \left(\frac{\sqrt{3}\angle -30}{(X+1+Y)}\right)
\end{aligned} \tag{20}$$

For the following formulas, we use the substitutions shown in (21) to place all impedances in per unit of the line impedance (ZL1).

$$X = \frac{ZS1}{ZL1}, 1 = \frac{ZL1}{ZL1}, Y = \frac{ZR1}{ZL1}, Z = \frac{ZRn_{Reach}}{ZL1} \tag{21}$$

B. Directional Elements

In this section, we provide the system conditions at which a directional comparison scheme that utilizes directional elements misoperates when a positive-sequence memory voltage expires.

1) R1 Direction Forward (No Memory)

The replica current at R1 is at an angle of 150 degrees (see Fig. 5). For the case in which the memory voltage has fully expired, R1 declares forward when the V1 angle evaluates to more than 60 degrees. In (22), we solve for the conditions at which the angle of V1R1 is more than 60 degrees.

$$\begin{aligned}
&V1R1 = \frac{X+(1+Y)\angle 120}{X+1+Y}\\
&60° < \arg\left(\frac{X+(1+Y)\angle 120}{X+1+Y}\right)\\
&60° < \tan^{-1}\left(\frac{(1+Y)\sin 120}{X+(1+Y)\cos 120}\right)\\
&\sqrt{3} < \left(\frac{(1+Y)\bullet\frac{\sqrt{3}}{2}}{X+(1+Y)\bullet\frac{-1}{2}}\right)\\
&X+(1+Y)\bullet\frac{-1}{2} < (1+Y)\bullet\frac{1}{2}\\
&-1 > -X+Y\\
&Y+1 > X\\
&ZR1+ZL1 > ZS1
\end{aligned} \tag{22}$$

2) R2 Direction Forward (No Memory)

The replica current at R2 is at an angle of –30 degrees (see Fig. 5). For the case in which the memory voltage has fully expired, R2 declares forward when the V1 angle evaluates to less than 60 degrees. In (23), we solve for the conditions at which the angle of V1R2 is less than 60 degrees.

$$\begin{aligned}
&V1R2 = \frac{X+1+Y\angle 120}{X+1+Y}\\
&60° > \arg\left(\frac{X+1+Y\angle 120}{X+1+Y}\right)\\
&60° > \tan^{-1}\left(\frac{Y\sin 120}{X+1+Y\cos 120}\right)\\
&\sqrt{3} > \left(\frac{Y\bullet\frac{\sqrt{3}}{2}}{X+1-Y\bullet\frac{1}{2}}\right)\\
&X+1-Y\bullet\frac{1}{2} > Y\bullet\frac{1}{2}\\
&X+1 > Y\\
&ZS1+ZL1 > ZR1
\end{aligned} \tag{23}$$

When the inequality statements shown in (22) and (23) are true, each terminal sees a forward fault once memory expires. This occurs when ZL1 is much larger than ZS1 and ZR1.

C. Distance Elements

In this section, we provide the minimum reach at which the R1 and R2 positive-sequence memory-polarized distance elements operate for a three-phase cross-connect fault.

1) R1 Mho (Reverse Zone)

In (24), we define the operate signal (SOP) for a reverse-looking zone and recall the positive-sequence voltage and current seen at Relay R1.

$$\begin{aligned} &SOP = -I1R1_{Replica} \bullet \left|ZR1_{Reach}\right| - V1R1 \\ &V1R1 = \left(\frac{X + (1+Y) \bullet 1\angle 120}{X+1+Y}\right) \\ &I1R1_{Replica} = -\frac{\sqrt{3}\angle -30}{X+1+Y} \end{aligned} \tag{24}$$

In (25), we plug V1R1 and I1R1 into SOP and simplify. If we assume SPOL is at 0 degrees, we know that the balance point for a distance element is when SOP is at 90 degrees (see (10)). If we take the real component of SOP and set it equal to zero, we can solve for the minimum reach required for a mho element operation based on the system conditions.

$$\begin{aligned} &\left|SOP_{ANG}\right| = 90 = \arg\left(\sqrt{3}\angle -30 \bullet Z - \left(X + \left(1+Y\right) \bullet 1\angle 120\right)\right) \\ &SOP_{Real} = 0 = \sqrt{3}\cos(-30) \bullet Z - \left(X + \left(1+Y\right)\cos\left(120\right)\right) \\ &0 = 1.5 \bullet Z - \left(X + \left(1+Y\right) \bullet \frac{-1}{2}\right) \\ &Z = \frac{X - \frac{Y+1}{2}}{1.5} \\ &ZR1_{Reach} = \frac{ZS1 - \frac{ZR1 + ZL1}{2}}{1.5} \end{aligned} \tag{25}$$

2) R2 Mho (Forward Zone)

In (26), we define the operate signal for a forward-looking zone and recall the positive-sequence voltage and current seen at Relay R2.

$$\begin{aligned} &SOP = I1R2_{Replica} \bullet \left|ZR2_{Reach}\right| - V1R2 \\ &V1R2 = \left(\frac{X+1+Y \bullet 1\angle 120}{X+1+Y}\right) \\ &I1R2_{Replica} = \frac{\sqrt{3}\angle -30}{X+1+Y} \end{aligned} \tag{26}$$

In (27), we plug V1R2 and I1R2 into SOP and simplify. If we assume SPOL is at 0 degrees, we know that the balance point for a distance element is when SOP is at 90 degrees (see (10)). If we take the real component of SOP and set it equal to zero, we can solve for the minimum reach required for a mho element operation based on the system conditions.

$$\begin{aligned} &\left|SOP_{ANG}\right| = 90 = \arg\left(\sqrt{3}\angle -30 \bullet Z - \left(X+1+Y \bullet 1\angle 120\right)\right) \\ &SOP_{Real} = 0 = \sqrt{3}\cos(-30) \bullet Z - \left(X+1+Y\cos\left(120\right)\right) \\ &0 - 1.5 \bullet Z - \left(X+1+Y \bullet \frac{-1}{2}\right) \\ &Z = \frac{X - \frac{Y}{2} + 1}{1.5} \\ &ZR2_{Reach} = \frac{ZS1 - \frac{ZR1}{2} + ZL1}{1.5} \end{aligned} \tag{27}$$

VII. References

[1] J. Larson and R. McDaniel, "Man-Made Faults – Line Protection Operation for an Unintended Phase Cross-Connect Condition," *2016 69th Annual Conference for Protective Relay Engineers (CPRE)*, April 2016, pp. 1–15.

[2] E. O. Schweitzer, III, and J. Roberts, "Distance Relay Element Design," proceedings of the 19th Annual Western Protective Relay Conference, Spokane, WA, October 1992.

[3] E. O. Schweitzer, III, "New Developments in Distance Relay Polarization and Fault Type Selection," proceedings of the 16th Annual Western Protective Relay Conference, Spokane, WA, October 1989.

[4] D. Hou, "Relay Element Performance During Power System Frequency Excursions," *2008 61st Annual Conference for Protective Relay Engineers*, 2008, pp. 105–117.

[5] R. Chowdhury and N. Fischer, "Transmission Line Protection for Systems With Inverter-Based Resources," proceedings of the 74th Annual Conference for Protective Relay Engineers, College Station, TX, March 2021.

[6] J. Roberts, A. Guzmán, and E. O. Schweitzer, III, "Z = V/I Does Not Make a Distance Relay," proceedings of the 20th Annual Western Protective Relay Conference, Spokane, WA, October 1993.

[7] M. J. Thompson and D. L. Heidfeld, "Transmission Line Setting Calculations – Beyond the Cookbook," *2015 68th Annual Conference for Protective Relay Engineers*, March 2015, pp. 850–865.

[8] R. Poduval, R. McDaniel, and S. Dasgupta, "Switch Onto Fault: Maintaining Dependability, Security and Speed," proceedings of the 47th Annual Western Protective Relay Conference, Virtual Format, October 2020.

[9] *SEL-T401L Ultra-High-Speed Line Relay Instruction Manual*. Available: selinc.com.

[10] M. J. Thompson, "Percentage Restrained Differential, Percentage of What?" *2011 64th Annual Conference for Protective Relay Engineers*, April 2011, pp. 278–289.

[11] B. Edwards, D. G. Williams, A. Hargrave, M. Watkins, and V. K. Yedidi, "Beyond the Nameplate – Selecting Transformer Compensation Settings for Secure Differential Protection," *2017 70th Annual Conference for Protective Relay Engineers (CPRE)*, April 2017, pp. 1–23.

[12] A. Guzmán, H. Altuve, and D. Tziouvaras, "Power Transformer Protection Improvements With Numerical Relays," proceedings of the CIGRE Study Committee B5 Colloquium, Calgary, Canada, September 2005.

[13] W. K. Sonnemann, C. L. Wagner, and G. D. Rockefeller, "Magnetizing Inrush Phenomena in Transformer Banks," *Transactions of the American Institute of Electrical Engineers. Part III: Power Apparatus and Systems*, Vol. 77, No. 3, April 1958, pp. 884–892.

[14] S. Hodder, B. Kasztenny, N. Fischer, and Y. Xia, "Low Second-Harmonic Content in Transformer Inrush Currents – Analysis and Practical Solutions for Protection Security," *2014 67th Annual Conference for Protective Relay Engineers*, March 2014, pp. 705–722.

[15] K. Behrendt, N. Fischer, and C. Labuschagne, "Considerations for Using Harmonic Blocking and Harmonic Restraint Techniques on Transformer Differential Relays," proceedings of the 33rd Annual Western Protective Relay Conference, Spokane, WA, October 2006.

[16] S. H. Horowitz and A. G. Phadke, *Power System Relaying*, 4th ed., Wiley, 2014.

[17] Central Station Engineers of Westinghouse, *Electrical Transmission and Distribution Reference Book*, 4th ed., Westinghouse Electric Corporation, 1964.

[18] X.-N. Lin and P. Liu, "The Ultra-Saturation Phenomenon of Loaded Transformer Energization and Its Impacts on Differential Protection," *IEEE Transactions on Power Delivery*, Vol. 20, No. 2, April 2005, pp. 1,265–1,272.

[19] A. Wiszniewski, W. Rebizant, D. Bejmert, and L. Schiel, "Ultrasaturation Phenomenon in Power Transformers—Myths and Reality," *IEEE Transactions on Power Delivery*, Vol. 23, No. 3, July 2008, pp. 1,327–1,334.

[20] M. Thompson and B. Kasztenny, "New Inrush Stability Algorithm Improves Transformer Protection," proceedings of the 14th International Conference on Developments in Power System Protection, Belfast, United Kingdom, March 2018.

[21] *SEL-487E-3, -4 Transformer Protection Relay Instruction Manual*. Available: selinc.com.

[22] R. Chowdhury, D. Finney, N. Fischer, and D. Taylor, "Determining CT Requirements for Generator and Transformer Protective Relays," proceedings of the 46th Annual Western Protective Relay Conference, Spokane, WA, October 2019.

VIII. Biographies

Marcel Taberer joined Schweitzer Engineering Laboratories, Inc. (SEL) as an application engineer in 2016. He previously worked for Eskom power utility in South Africa as a protection engineering technologist for 9 years. He was responsible for commissioning and testing primary and secondary plant equipment in the distribution and transmission sector within the Eastern Cape. He earned his Bachelor of Technology degree from Cape Peninsula University of Technology and his Master of Technology degree from Nelson Mandela Metropolitan University. Marcel is a senior IEEE member and a registered professional engineer in the state of Texas.

Ryan McDaniel earned his BS in computer engineering from Ohio Northern University in 2002. In 1999, he was hired by American Electric Power (AEP) where he worked as a relay technician and a protection and control engineer. In 2005, he joined Schweitzer Engineering Laboratories, Inc. (SEL) and is currently a principal engineer. His responsibilities include providing application support and technical training for protective relay users. Ryan is a registered professional engineer in the state of Illinois and a member of IEEE.

Jon Larson is an application engineer in protection with Schweitzer Engineering Laboratories, Inc. (SEL) and is located in Marshall, Michigan. Jon received BSEE and MSEE degrees from Michigan Technological University and an MBA from Eastern Michigan University. For 15 years, he worked at a major Midwest utility with responsibilities primarily in protective relaying. He has been employed with SEL since October 2002. Jon is a member of IEEE and a registered professional engineer in the state of Michigan.